BOLETIN DE LA SOCIEDAD ESPAÑOLA DE
Cerámica y Vidrio
www.elsevier.es/bsecv

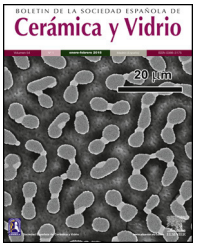

Alternative technological approach for synthesis of ceramic pigments by waste materials recycling

Mihail Doynov[a], *Tsvetan Dimitrov*[b], *Stephan Kozhukharov*[c,*]

[a] *LUKOIL Neftochim Burgas Co, 8014 Burgas, Bulgaria*
[b] *Rousse University "Angel Kanchev", Razgrad Branch, 47 "Aprilsko vastanie" Blvd., Razgrad 7200, Bulgaria*
[c] *University of Chemical Technology and Metallurgy, 8 "Klyment Okhridsky" Blvd., Sofia 1756, Bulgaria*

ARTICLE INFO

Article history:
Received 16 September 2015
Accepted 12 January 2016
Available online 1 February 2016

Keywords:
Chromspinelides
Ceramic pigments
Industrial wastes

ABSTRACT

Alternative technological approach is proposed enabling utilization of raw materials from an oil refinery, such as waste guard layers from reactors. Reagent grade and purified MgO, Cr_2O_3, Fe_2O_3, and nitric acid (HNO_3), were used as additional precursors. The homogeneous mixtures obtained were formed into pellets and sintered at different temperatures. The main phase was proved by X-ray phase analysis (XRD) and compared to ICPDS database. The main phase in the ceramics synthesized was solid solution of spinel $MgAl_2O_4$ and magnesiochromite. These minerals are classified as chromspinelide $MgCr_{1.2}Al_{0.4}Fe_{0.4}O_4$ and alumochromite $MgCr_{1.6}Al_{0.4}O_4$. Additional SEM observations, combined with EDX analysis were performed, evincing agglomeration at lower temperatures, followed by agglomerate crumbling, at elevated calcination temperature.

The complete transformation of initial precursors into the final ceramic compounds was found to occur at 800 °C – 1 h. The ceramic samples synthesized had high density of 1.72–1.93 g/cm^3 and large absorption area – 32.93% which is probably due to the high porosity of the sample.

Método tecnológico alternativo de síntesis de pigmentos cerámicos a partir de reciclaje de materiales provenientes de residuos

Palabras clave:
Espinelas del cromo
Pigmentos cerámicos
Materiales de desecho industriales

RESUMEN

En este trabajo se propone un método para el aprovechamiento de materiales provenientes de residuos de las refinerías de petróleo, utilizando para ello los desechos de las capas protectoras de los reactores químicos. Usando como precursores adicionales, reactivos de alta pureza tales como MgO, Cr_2O_3, Fe_2O_3, y ácido nítrico (HNO_3), se han preparado mezclas homogéneas en forma de pastillas, que se han sometido calcinadas a diferentes temperaturas. Las fases obtenidas han sido analizadas mediante difractometría de rayos X. La fase dominante de los pigmentos cerámicos obtenidos está compuesta por una solución sólida de tipo espinela $MgAl_2O_4$ y cromato de magnesio. Esos productos se clasifican como espinelas

* *Corresponding author.*
E-mail address: stephko1980@abv.bg (S. Kozhukharov).
http://dx.doi.org/10.1016/j.bsecv.2016.01.002

de cromo $MgCr_{1.2}Al_{0.4}Fe_{0.4}O_4$ y cromato de aluminio $MgCr_{1.6}Al_{0.4}O_4$. Adicionalmente, se han realizado observaciones mediante microscopia electrónica de barrido combinada con análisis químico por energías dispersivas de rayos X. Los materiales resultantes presentan aglomerados debido a las bajas temperaturas de calcinación. Se ha establecido que después de una exposición a 800 °C durante una hora, los precursores se transformaron completamente en pigmentos cerámicos. Los pigmentos cerámicos obtenidos poseen una alta densidad en el rango de 1,85 a 2,60 g/cm^3 y una porosidad abierta entre 28,9 y 32,93% a 700 °C.

Introduction

Although the traditional production of spinels is based on the use metallic oxides as raw materials [1], the use of non-conventional precursors enables spinels synthesis at lower temperatures, decreasing, in general the energy demands for their industrial production. This approach was successfully applied for synthesis of $MgAl_2O_4$ from Al and Mg compounds and triethyl amine [2]. Common spinel has been formed after heating the mixture to 675 °C, resulting in crystal size was about 20 nm. Spinel pigments based on $CaFe_2O_4$ have been successfully elaborated by Candeia et al. [3], using polymeric precursor method, via polymerization of citric acid in medium of ethylene glycol. The metallic ion containing precursors used for the pigment synthesis were $Fe(NO_3)_3$ and $(CH_3COO)_2Ca$. Pigments with non-stochiometric composition, corresponding to general formula Me_2YnO_{2n-2} with various chromophores assigned as "Me", such as Fe, Zn, Ni, Mg, Cu, Co and Mn, added in molar portions: $n = 0.3–2.5$ are already patented [4]. Combustion method is used by Deraz and co. [5] in order to obtain a spinel structured pigments, composed by magnesium ferrite solid solution with iron-rich composition, $MgFe_2O_4 \cdot xFe_2O_3$. Besides the iron, the chromium also appears an important widely investigated chromophoric ingredient [6–13]. In this sense, Díaz et al. propose synthesis of ferrite spinel [14] on the basis of steel waste as iron source.

Another trend of great importance for the ceramic industry, object of recently increasing interest is the recycling of waste materials from other industrial branches [14–19]. Besides, even some natural products as silica from rise husks have been recently employed for ceramic materials production [20–27].

Spinel powder with composition $Zn_{1-x}Cd_xCr_2O_4$, where $0 \leq x \leq 1$, has been synthesized by thermal decomposition of nitrates, at relatively low temperature interval between 600 and 800 °C, and the obtained material was characterized by XRD and SEM [28]. Other authors have been used the combustion of preliminary obtained sol–gel products for elaboration of nanometric powder materials, based on the system $ZnO–TiO_2–V_2O_5$ [29–31].

Similar approach has been used for synthesis of stoichiometric $MgAl_2O_4$ spinel, by pyrolysis in air of $Al(OH)_3$ and MgO dissolved in triethylamine [32]. The metal compounds were found to decrease the temperature of beginning of synthesis by 200 °C compared to the conventional synthesis from $Al(OH)_3$ and MgO [33,34].

Smirnov et al. [35] have used flame pyrolysis as a method for synthesis of Alumochrome spinel and $MgAl_2O_4$ powders. In both cases, aqueous solution of $Mg(NO_3)_2$ and $Al(NO_3)_3$ was ignited in the upper zone of an electric oven at 900 °C. The composition of the former powder obtained was 93.36 mol% – $MgAl_2O_4$ and 6.64 mol% Y_2O_3, whereas the latter composite spinel material contained 75.75 mol% $MgAl_2O_4$. The obtained composite materials were with 2 μm particle size, accompanied with needle-like crystals. After subsequent wet grinding, followed by annealing at 1700 °C for10 h, spinel ceramics with relative density about 97.6% of the theoretical one was prepared.

Other authors [36,37] have performed comparative research on the correlation between the synthesis conditions and the microstructure of ceramic materials from the $Al_2O_3–MgO–ZrO_2$ system. As a main result, the authors have established that the increase of MgO content results in increased microhardness, due to recrystallization.

Using the method of co-precipitation, spinel was synthesized and the influence of the process on the synthesis temperature was studied. The initial aqueous solutions of Mg and Al nitrates were mixed with water-insoluble polymer "laxsin" and co-precipitated to obtain a mixture of carbonates. The precipitate was filtered after 12 h period of maturing and then heated to 1300 °C [38]. The spinel was reported to form at 1000 °C.

Other authors have studied the effect of synthesis conditions on the parameters of the process of spinel ceramics synthesis [39]. To obtain fine powder, the method of co-precipitation from concentrated solutions was used which allowed increasing the reactivity of the interacting substances. Sulfides of magnesium and aluminum were used. The components were precipitated in 25% aqueous solution of ammonium under continuous stirring at room temperature and pH = 9–9.5. The precipitate obtained was dried and then heated in sillite oven at temperatures 1000–1300 °C at temperature increase rate of 150 °C/h. Recently, Nazarkovsky et al. [40] have used hydrothermal and solvothermal methods for synthesis of powder shaped ceramics, such as Cu(II) and Ni(II) doped SiO_2-TiO_2 nanocomposites, and Sn doped titania [41]. Similar approach is used for development of kesterite based materials for photovoltaic elements as exterior building tiles [42,43]. Besides as components of high performance photovoltaics, the powder ceramic materials encounter continuously increasing applications for solid oxide fuel cells [44–46], environmental sensor elements [47,48] and even for corrosion protection [49,50].

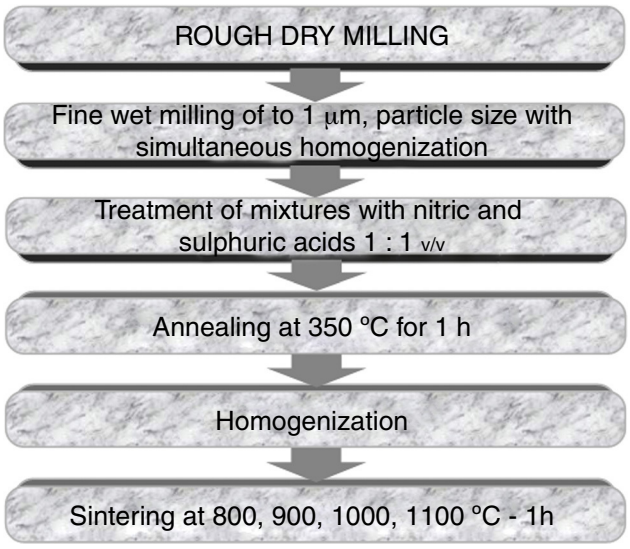

Fig. 1 – Technological scheme for synthesis of ceramics from industrial waste materials from oil refining.

The ceramics sintering conditions are very important for the formation of the spinel structure [51], especially the temperature and isothermal period [52].

Following these actual trends of the modern ceramic industry, the present research work is devoted on the elaboration of alternative ceramic pigments, prepared by application of waste materials from the oil refinery industry. Besides, a comparative research is performed on the sintering temperature impact on the morphology and the stability of the obtained pigments.

Experimental

Sample preparation

The compositions of the investigated samples were prepared by mixing of MgO, and Al_2O_3. Fe_2O_3 and Cr_2O_3 from waste products of the refinery industry were used as chromophores. The obtained mixtures were sintered in temperature interval between 700 and 1100 °C for one hour. The subsequence of the technological procedures for complete conversion of the initial precursor mixtures to resulting pigments is depicted in Fig. 1.

Characterization of the obtained pigments

Colorimetric measurements were performed by "Lovibond TR – 100". The water uptake capability W%, and the apparent density D% were determined by pycnometer, following systematic procedures by weighting before and after distilled water addition, and subsequent drying at 120 °C for 2 h. In order to determine the grain size of the obtained powder products comparative observations by Scanning Electron Microscopy (SEM), were performed, TESCAN, SEM/FIB LYRA I XMU with 30 kV acceleration, at different resolutions,

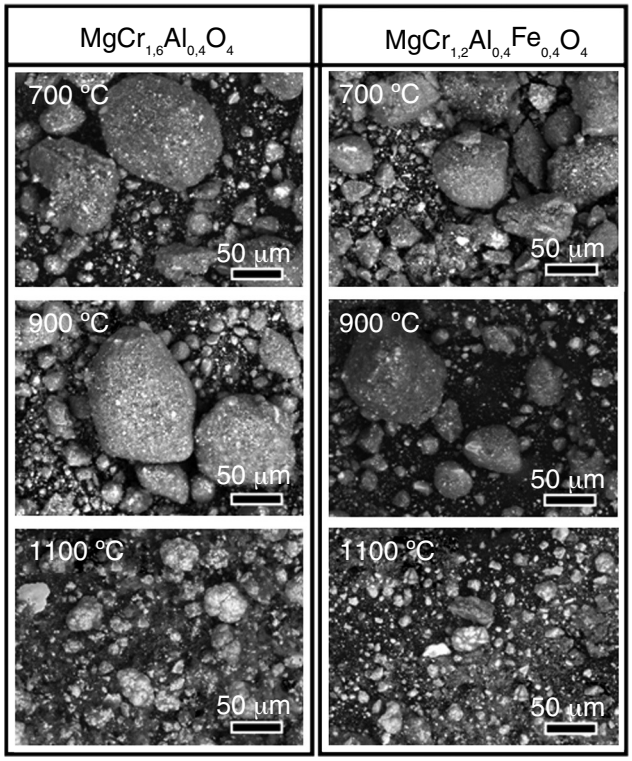

Fig. 2 – Systematic SEM observations on selected specimens, acquired at magnification 1000×.

combined with Energy Dispersion Spectrometer (Quantax 200 of BRUKER detector).

The obtained ceramic materials were characterized by structural analysis via XRD, from 10° to 70° angular, with XRD "PHILIPS"-APD-15, CuKα diffractometer.

Results and discussions

Systematic SEM observations

Undoubtedly, the temperature has a great impact on the structure, and morphology of the obtained ceramic materials. That was the reason for the systematic comparative observation on the morphologies of the obtained ceramic pigments according to both of their composition and calcining temperature. In this sense, powder samples from both investigated compositions: $MgCr_{1.6}Al_{0.4}O_4$ and $MgCr_{1.2}Al_{0.4}Fe_{0.4}O_4$, sintered at 700, 900 and 1100 °C were submitted to observations via SEM. The obtained images are shown in Fig. 2.

The images in Fig. 2 reveal that at lower temperatures in the range between 700 and 900 °C the obtained powders with both compositions possess highly agglomerated morphology. Besides the large oval agglomerates with average dimensions of about 100–150 μm, there is a presence of smaller coarse particles with size dimensions between 10 and 40 μm. On the other hand, obviously the further temperature elevation up to 1100 °C results to crumbling of the large sized agglomerates. Besides, there is simultaneous presence of brighter and darker resulting smaller particles with undoubtedly distinguishable compositions. Indeed, the subsequent EDX analyses

Table 1 – Colorimetric indexes of pigments calcined at 700 and 1100 °C.

$MgCr_{1.6}Al_{0.4}O_4$					
700 °C			1100 °C		
L^*	a^*	b^*	L^*	a^*	b^*
64.73	−4.55	15.12	78.20	−1.37	14.04
$MgCr_{1.2}Al_{0.4}Fe_{0.4}O_4$					
700 °C			1100 °C		
L^*	a^*	b^*	L^*	a^*	b^*
54.28	13.12	24.80	52.65	15.97	24.53

(not shown in the figures) have revealed that the larger brighter particles contain a larger amount of aluminum, whereas the darker coarse ones contain superior quantity either of Cr or Fe. Finally, it is worth to mention that the particles of the pigment, prepared with addition of iron are relatively smaller, than the composition prepared without iron addition. The most probable reason for this phenomenon is that the supplemental iron induces more intensive point defects diffusion. As consequence, these point defects heap on the grain boundaries of the oxide crystallites causing significant mechanical tensions among the oxide crystals composing the agglomerates, formed at lower temperatures. Indeed, the supplemental Fe_2O_3 undergoes a phase transition to unstable wustite ($Fe_{x-1}O$) phase at 570 °C [53,54]. This cation deficient oxide is described in the literature as a p-type semiconductor that enables diffusion of cationic vacancies and holes. Besides, at high temperatures this phase coexists with other Fe-O phases, such as Fe_3O_4 (magnetite) and Fe_2O_3 (hematite), and even the so called "inverted spinel", ($FeFe_2O_4$), $FeCr_2O_4$. In addition, the hematite layer is porous and thus, oxygen gas permeable phase that allows oxygen penetration and subsequent reduction into O^{2-} on the magnetite-hematite interface [55]. Such processes lead to further densification of the agglomerates, accompanied by agglomerate shrinking. The coexistence of several Fe–O phases with active superficial ion-exchange processes on the grain boundaries predetermines stronger high temperature mechanical tensions on the grain boundaries among the particles, consisting the respective agglomerates. Additional very probable reason for the lower size of these pigment particles is that the simultaneous presence of various iron oxides with distinguishable thermal expansion coefficients imposes supplemental mechanical tensions, resulting in relatively smaller agglomerates, compared with the other composition.

Similar phenomena happen in the case of $MgCr_{1.6}Al_{0.4}O_4$. Again, the EDX analyses reveal irregular distribution of the composing elements, revealing the simultaneous presence of various oxides, such as Cr_2O_3, CrO_3, $MgAl_2O_4$, etc. In the basic phase, $MgCr_{1.6}Al_{0.4}O_4$ the chromium and aluminum cations render a partial positive charge to the MgO crystals. Thus, these oxides cause a higher affinity to oxygen, predetermining a non-stoichiometry, ion diffusion and consequently – stronger Van der Waals attraction among the crystals, composing the resulting agglomerates. That is the reason for the remarkable size of the agglomerates, observed for the non-doped composition, for the 700–900 °C temperature range.

Finally, although the extraordinary high melt point of the corrundum, both the compositions sintered at 1100 °C reveal presence of irregularly shaped oval particles with ellipsoidal Al-inclusions, evincing that the commented above oxides predetermine reductive medium, which consume the oxygen from the Al_2O_3 phase. Thus, the remaining excessive aluminum suffers melting, followed by precipitation of the Al-melt in the aggregates, and subsequent solidification of metallic aluminum.

Regardless the sharp change of the sample's morphology at 1100 °C, it was not accompanied by significant variations in their color-related properties, as is demonstrated in the following section.

Colorimetric measurements

For determination of the impact of the calcination temperature on the color of the obtained pigments, colorimetric measurements have been performed. Surprisingly, the respective results have shown that the sharp alteration of the sample's morphology does not lead to notable color changes of the respective pigments. Indeed, Table 1 reveals almost identical values of the colorimetric data for the specimens, sintered at 700 and 1100 °C.

The measurements were performed according the CIE-L^*, a^*, b^* [56]. The results completely confirm that the color difference is rather consequence of the pigment composition, than result of the calcination temperature. Indeed, all the $MgCr_{1.6}Al_{0.4}O_4$ pigments possess greenish color, whereas the iron contributes for the reddish colorization of the doped pigments $MgCr_{1.2}Al_{0.4}Fe_{0.4}O_4$, and the colors remain almost unchanged irrespective the calcination temperature. The former composition reveals a slight increase of the brightness values L^*, combined with insignificant decrease of the green component a^* values with increase of the treatment temperature. At the same conditions, the later, iron containing composition, the values of L^* and b^* remain almost the same, whereas the reddish component a^* suffers negligible enhancement, revealing either transition of Cr(III) to Cr(IV) due to oxidation, or formation of pure red Fe_2O_3 fraction. The latter is much more probable, because the Cr(IV) is extremely instable, and converts to yellow Cr(VI)-compounds.

Table 2 – Water uptake capability (W%), and apparent density (D%) values acquired for $MgCr_{1.6}Al_{0.4}O_4$ and $MgCr_{1.2}Al_{0.4}Fe_{0.4}O_4$ calcined for 1 h either at 700 or at 1100 °C $MgCr_{1.6}Al_{0.4}O_4$.

Chemical composition	Calcination temperature (°C)	W% (%)	D% (g/cm^3)
$MgCr_{1.6}Al_{0.4}O_4$	700	32.9342	1.9282
	1100	28.0250	2.5620
$MgCr_{1.2}Al_{0.4}Fe_{0.4}O_4$	700	35.6320	1.8562
	1100	28.8965	2.6032

Table 3 – Comparison between the lattice parameters of $MgCr_{1.6}Al_{0.4}O_4$, samples calcined either at 700 or at 1100 °C, with ICDD data for Mg-Al spinel.

$MgCr_{1.6}Al_{0.4}O_4$ Calcined at 700 °C			$MgCr_{1.6}Al_{0.4}O_4$ Calcined at 1100 °C			Spinel 03-0901	
d. 10 (nm)	I/I_1 (%)	*hkl*	*d*. 10 (nm)	I/I_1 (%)	*hkl*	*d* (Å)	I/I_1 (%)
4.88	30	111	4.65	20	111	4.68	50
3.70	40	211	3.70	40	300	–	–
3.17	100	310	3.16	100	221	3.35	10
2.82	40	222	2.84	70	222	2.83	50
2.60	50	421	2.62	40	421	–	–
2.54	30	311	2.54	30	311	2.43	100
2.31	10	400	2.21	30	400	–	–
2.02	40	400	2.02	20	400	2.02	80
1.65	20	422	1.66	20	422	1.65	30
1.58	20	511	1.48	10	511	1.55	30

The contraversion between the inference from the SEM observations, that at 1100 °C, the samples suffer complete morphological change, and the lack of notable color alteration leads to the conclusion that there are not remarkable phase transitions in their compositions, but rather gradual phase transitions, as is pointed below. The agglomerate crumbling at the highest investigated temperature is either result of the thermal expansion coefficient difference among the composing oxides, or due to cracking originated from point defect diffusion. Another possible reason for the agglomerate crumbling at 1100 °C is the intensive evaporation of adsorbed water at this high temperature, that lead to elevation of the pressure inside the pores causing agglomerate splitting. The phase stability of the respective pigments reveals that these ceramics can be obtained at 700 °C enabling lower energy spends for their production.

Characterization of physical chemical properties

The elaboration of appropriated technological cycles in the ceramic industry demand determination of various mechanical and physical-chemical properties. Besides the color parameters, the usability of the ceramic pigments is predetermined by other properties, such as wettability (i.e. water uptake capability) W%, and the apparent density D%. These parameters are evaluated for specimens from both the investigated compositions, sintered at 700 and 1100 °C, and their values are shown in Table 2.

The comparison of the values shown in Table 2 reveals that the addition of Fe to the pigment composition does not affect considerably neither the apparent density, nor the water uptake capability. The D% values for both compositions calcined at 700 °C, reaches about 2 g/cm^3, whereas the higher calcination temperature (i.e. 1100 °C), results in density increase to above 2.5 g/cm^3. The water uptake capability of both compositions investigated slightly decreases with increase of the calcination temperature with about 5%, due probably to phase transitions inside the pigment particles, or decomposition of chemically bonded superficial hydroxide layer.

The higher calcination temperatures lead to lower W% values, due to destruction of the large sized agglomerates, commented in "Systematic SEM observations" section. These formations probably possess a developed porosity, which enhances the water uptake capability. However, the thermal treatment at 1100 °C promotes intensive water evaporation and consequent agglomerate splitting, due to the water vapors' pressure. As a result, the finer pigment fractions obtained at 1100 °C (Fig. 2) possess identical water absorption (i.e. W%) values, between 28, and 29%, due to the identical surface roughness obtained.

At 700 °C, the corresponding compositions possess lower density values, compared to these of the specimens sintered at 1100 °C. This effect coincides the agglomerate crumbling, observed by the SEM observations. Consequently, at this temperature, the large size agglomerates really suffer crumbling due to evaporation of the adsorbed water, resulting in finer and denser dispersive particles. In order to establish whether the agglomerate splitting is coincided by any phase transitions, additional XRD studies were performed, and the respective results are shown below.

XRD structural characterization

The XRD patterns, shown in Table 3, for $MgCr_{1.6}Al_{0.4}O_4$, calcined either at 700, or at 1100 °C, reveals occurrence of residual

Table 4 – Comparison between the lattice parameters of $MgCr_{1.2}Al_{0.4}Fe_{0.4}O_4$, samples calcined either at 700 °C or at 1100 °C, with ICDD data for Mg-Al spinel.

$MgCr_{1.2}Al_{0.4}Fe_{0.4}O_4$ calcined at 700 °C			$MgCr_{1.2}Al_{0.4}Fe_{0.4}O_4$ calcined at 1100 °C			Spinel 03-0901	
d. 10 (nm)	I/I_1 (%)	*hkl*	*d*. 10 (nm)	I/I_1 (%)	*hkl*	*d* (Å)	I/I_1 (%)
3.70	20	111	4.70	30	111	4.68	50
3.63	10	121	4.64	10	122	–	–
3.16	100	211	3.38	100	130	3.35	10
2.84	70	222	2.84	80	222	2.83	50
2.60	20	240	2.63	30	240	–	–
2.21	40	311	2.43	20	311	2.43	100
2.08	10	400	2.11	20	322	–	–
2.02	20	400	2.03	10	400	2.02	80
1.81	30	422	1.65	30	422	1.65	30
1.48	10	511	1.51	10	511	1.55	30

Cr_2O_3 and α-Al_2O_3, accompanied by traces of nano-crystalline MgO, below 2%. However, the basic compound of both the samples is $MgCr_{1.6}Al_{0.4}O_4$, which can be assumed as a solid solution of spinel ($MgAl_2O_4$) ICDD PDF 5-0672 (0.284 (62)–0.243 (2)–0.202 (7)–0.142 (5)) and magnesium chromite ($MgCr_2O_4$) ICDD PDF 10-0351: (0.481 (4)–0.251 (16)–0.208 (24)–0.147 (11)).

A peak was observed at 0.316 (100) and it corresponds to a solid solution of $MgAl_2O_4$ and $MgCr_2O_4$, being in form of magnesium alumochromite. Indeed, the minerals from the spinel and the magnetite-chromite groups possess unlimited miscibility among themselves. The stoichiometric calculations in this case show that the resulting alumochromite is composed by about 80% magnesium chromite and 20% spinel phase. At temperatures above 1000 °C complete mixing of the solid solutions is already observable in form of pure magnesium alumochromite phase.

Both the iron containing compositions, calcined at 700 and 1100 °C are basically composed by $MgCr_{1.2}Al_{0.4}Fe_{0.4}O_4$, which is in form of solid solution of spinel ($MgAl_2O_4$) ICDD PDF 5-0672 (0.284 (62)–0.243 (2)–0.202 (7)–0.142 (5)), magnesium chromite ($MgCr_2O_4$) ICDD PDF 10-0351: (0.481 (4)–0.251 (16)–0.208 (24)–0.147 (11)) and magnesium ferrite ($MgFe_2O_4$) ICDD PDF 01-1120: 0.251(10)–0.295(4)–0.148(3), shown in Table 4.

Besides, the peak at 0.316 (100) of the XRD pattern (not shown in the figures) belongs to magnesium alumochromite. At temperatures above 1000 °C, this phase almost completely (i.e. with 92%) converts to magnesium chromite. The overlapping between the peaks of both these minerals originates from the identical structural ordering of their crystalline lattices possessed by both the magnesium chromite and alumochromite minerals.

Conclusions

A technological scheme for synthesis of ceramic materials by employment of waste materials from oil refinery containing heavy metals is developed. It was found that the whole amount of heavy metals was bound into the chromspinelides obtained. The SEM images reveal that the pigments calcined at temperature interval between 700 and 900 °C, possess highly agglomerated morphology, whereas at 1100 °C, the already formed agglomerates undergo structural decomposition. The colorimetric measurements have revealed that the sharp morphological changes between 900 and 1100 °C, does not result in notable color alteration. This fact shows that the pigments obtained by the technological procedures, proposed in the present research work can be successfully calcined at lower temperatures, decreasing in general the energetic spends for their industrial production.

The physical chemical and structural investigations have revealed that the higher water adsorption capability of the large size agglomerates, formed below 900 °C, results in agglomerate splitting at 1100 °C, due to the intensive water evaporation, and the respective elevation of the water pressure inside the agglomerate pores.

Unexpectedly, the hardness of both the compositions investigated decreases with increase of the calcination temperature due probably to phase transitions inside the pigment particles. Indeed, the XRD patterns reveal phase transition of the solid solution of $MgAl_2O_4$ and $MgCr_2O_4$ to pure magnesium alumochromite phase at temperatures above 1000 °C, whereas for the iron containing compositions, almost completely (i.e. with 92%) converts to magnesium chromite at these temperatures. Consequently, the compositions, sintered at lower temperatures possess superior characteristics, as water uptake capability (W%), and apparent porosity (AP%), enabling their successful use in the ceramic industry.

As a general conclusion of the present research work, it can be inferred that the proposed alternative technological schedule provides economical production of ceramic pigments with remarkable compositional stability at relatively low temperature of calcination.

Acknowledgement

The present research work is realized on the basis of the financial support of Bulgarian National Scientific Fund, Contract T 02-27.

REFERENCES

[1] A.G. Riabuhin, Oxyde spinels type 2–4, Cheliabinsk Sci. Center 1 (2002) 26–28.
[2] G.N. Pirogova, N.M. Panich, R.I. Korosteleva, U.B. Voronin, Izv. RAN, Ser. Chem. (1996) 2666–2669.

[3] R.A. Candeia, M.I.B. Bernardi, E. Longo, I.M.G. Santos, A.G. Souza, Synthesis and characterization of spinel pigment $CaFe_2O_4$, obtained by the polymeric precursor method, Mater. Lett. 58 (2004) 569–572.
[4] R.A. Eppler, Orange pigments of spinel structure, European patent EP0059364 B1 (1984).
[5] N.M. Deraz, O.H. Abd-Elkader, Investigation of magnesium ferrite spinel solid solution with iron-rich composition, Int. J. Electrochem. Sci. 8 (2013) 9071–9081.
[6] S. Mestre, M.P. Gómez-Tena, M.F. Gazulla, A. Gozalbo, Interaction of the chromium–iron black pigment with porcelanised stoneware, Ceram. Int. 39 (2013) 7453–7459.
[7] Le Zhang, Zhenbang Pi, Chao Yang, Xike Tian, Synthesis of chromium-doped malayaite pigments from wastewater containing low chromium(VI), J. Air Waste Manage. Assoc. 60 (2010) 1257–1261.
[8] V. Harisanov, R.S. Pavlov, I.T. Marinova, V.S. Kozhukharov, J.B. Carda, Influence of crystallinity on chromatic parameters of enamels coloured with malayaite pink pigments, J. Eur. Ceram. Soc. 23 (2003) 429–435.
[9] E. López-Navarrete, M. Ocaña, A simple procedure for the preparation of Cr-doped tin sphene pigments in the absence of fluxes, J. Eur. Ceram. Soc. 22 (2002) 353–359.
[10] G. Costa, M.J. Ribeiro, J.A. Labrincha, M. Dondi, F. Matteucci, G. Cruciani, Malayaite ceramic pigments prepared with galvanic sludge, Dyes Pigm. 78 (2008) 157–164.
[11] E. Lopez-Navarrete, A. Caballero, V.M. Orera, F.J. Lázaro, M. Ocaña, Oxidation state and localization of chromium ions in Cr-doped cassiterite and Cr-doped malayaite, Acta Mater. 51 (2003) 2371–2381.
[12] E. López-Navarrete, A.R. González-Elipe, M. Ocaña, Non-conventional synthesis of Cr-doped SnO_2 pigments, Ceram. Int. 29 (2003) 385–392.
[13] V.P. Della, J.A. Junkes, C.R. Rambo, D. Hotza, Synthesis of the ceramic pigment victoria green ($Ca_3Cr_2Si_3O_{12}$) from $CaCO_3$, Cr_2O_3 and SiO_2, Quim. Nova 31 (2008) 1004–1007.
[14] G.C. Díaz, E.A. Reynoso, M.C. Castañon-Bautista, O. Novelo, R. Jordan, Synthesis of $MgFe_2O_4$ spinel using steel waste as iron resource, Int. J. Eng. Innov. Technol. 4 (2015) 1–4, ISSN:2277-3754.
[15] G. Costa, M.J. Ribeiro, J.A. Labrincha, Development of waste-based ceramic pigments, Bol. Soc. Esp. Ceram. Vidrio 46 (2007) 7–13.
[16] J.A. Durán Suárez, J. Montoya Herrera, A.P. Silva, R. Peralbo Cano, J.P. Castro-Gomes, Validación de nuevos materiales cerámicos a partir de rocas de desecho de minería. Propiedades mecánicas, Bol. Soc. Esp. Ceram. Vidrio 53 (2014) 279–288.
[17] G. Costa, V.P. Della, M.J. Ribeiro, J.A. Labrincha, Forming black spinel pigment from industrial sludge, Am. Ceram. Soc. Bull. 87 (2008) 9101–9107.
[18] D. Fraga, A. Gyozova, S. Kozhukharov, S. Allepuz, C. Lázaro, V. Trilles, J. Carda, Development of new ecological ceramic tiles by recycling of waste glass and ceramic materials, in: Annual Proceedings of Angel Kanchev University of Ruse, Bulgaria, 50 (9.1), 2011, pp. 8–12, Available at: http://conf.uni-ruse.bg/bg/docs/cp11/9.1/9.1-1.pdf.
[19] C. Munevver, K.S. Yesilay, G. Busra, The use of glass waste in stoneware glazes, Ceram. Techn. 37 (2013) 30–37, ISSN:1324-4175.
[20] M.I. Martín, J. Mª Rincón, F. Andreola, L. Barbieri, F. Bondioli, I. Lancellotti, M. Romero, Materiales vitrocerámicos del sistema MgO-Al_2O_3-SiO_2 a partir de ceniza de cáscara de arroz, Bol. Soc. Esp. Ceram. Vidrio 50 (2011) 201–206.
[21] F. Bondioli, F. Andreola, L. Barbieri, T. Manfredini, A.M. Ferrari, Effect of rice husk ash (RHA) in the synthesis of (Pr,Zr)SiO ceramic pigment, J. Eur. Ceram. Soc. 27 (2007) 3483–3488.
[22] T. Luangvaranunt, C. Dhadsanadhep, J. Umeda, E. Nisaratanaporn, K. Kondoh, Aluminum-4 mass% copper/alumina composites produced from aluminum copper and rice husk ash silica powders by powder forging, Mater. Trans. 51 (2010) 756–761.
[23] B.K. Ngun, H. Mohamad, E. Sakai, Z.A. Ahmad, Effect of rice husk ash and silica fume in ternary system on the properties of blended cement paste and concrete, J. Ceram. Process. Res. 11 (2010) 311–315.
[24] C. Real, M.D. Alcalá, J.M. Criado, Preparation of silica from rice husks, J. Am. Ceram. Soc. 79 (1996) 2012–2016.
[25] F. Bondioli, F. Andreola, L. Barbieri, T. Manfredini, A.M. Ferrari, Effect of rice husk ash (RHA) in the synthesis of (Pr,Zr)SiO ceramic pigment, J. Eur. Ceram. Soc. 27 (2007) 3483–3488.
[26] N. Yalçin, V. Sevinç, Studies on silica obtained from rice husk, Ceram. Int. 27 (2001) 219–224.
[27] C.S. Prasad, K.N. Maiti, R. Venugopal, Effect of substitution of quartz by rice husk ash and silica fume on the properties of whiteware compositions, Ceram. Int. 29 (2003) 907–914.
[28] Y.-H. Lei, Y.-B. Sun, Y.-Z. Cheng, Y.-R. Wang, L.-H. Xue, Sol–gel synthesis of normal spinel $LiMn_2O_4$ and its characteristics, J. Wuhan Univ. Technol. Mater. Sci. Ed. 17 (2002) 1–4.
[29] R. Gegova, Y. Dimitriev, A. Bachvarova-Nedelcheva, R. Iordanova, A. Loukanov, T.Z. Iliev, Combustion gel method for synthesis of nanosized ZnO/TiO_2 powders, J. Chem. Technol. Metall. 48 (2013) 14–153.
[30] A. Shalaby, A. Bachvarova-Nedelcheva, R. Iordanova, Y. Dimitriev, A study of the effect of citric acid on the crystallinity of ZnO/TiO_2 nanopowders, J. Chem. Technol. Metall. 48 (2013) 585–590.
[31] Y. Dimitriev, Y. Ivanova, A. Staneva, L. Alexandrov, M. Mancheva, R. Yordanova, C. Dushkin, N. Kaneva, C. Iliev, Synthesis of submicron powders of ZnO and ZnO-M_nO_m (M_nO_m = TiO_2, V_2O_5) by sol–gel methods, J. Univ. Chem. Technol. Met. (Sofia) 44 (2009) 235–242.
[32] B. Kamenov, Magmatic petrology, Unv. Publ., St. Kliment Ohridsky, Sofia, 25, (2003) 34–36.
[33] A.E. Ringwood, Composition and Petrology of the Earth's Mantle, Mc Graw-Hill, NY, 1975, pp. 618.
[34] A.E. Ringwood, A model for the upper mantle, J. G. R. 67 (1962) 857–867.
[35] V.I. Smirnov, M.D. Zhelyazkova-Panajotova, A.I. Ginzberg, V.M. Grigoriev, G.F. Yackovlev, Geology of ore deposits, Science and art, Sofia, 1986, pp. 48–59.
[36] D. Chin, D.B. Baruwati, S. Manorama, A simple chemical synthesis of nanocrystalline AFe_2O_4 (A = Fe, Ni, Zn): an efficient catalyst for selective oxidation of styrene, J. Mol. Catal. A: Chem. 242 (2005) 26–31.
[37] B. Locaci, Symposium on Nucleation and Crystallization in Glasses and Melts, and Palbl, Amer. Cer. Soc. Inc., Ohio, 1962, pp. 71–74.
[38] C.E. Rindone, Am. Ceram. Soc. 41 (1958) 141.
[39] V.U. Belousova, U.E. Pingvinskiy, I.V. Galenko, Intern Konf. prom-st stroymater. Building Industry and Energy and careful resource in rInoch. relations, Belgrad, 1997.
[40] M.A. Nazarkovsky, E.V. Goncharuk, E.M. Pakhlov, E. Skwarek, J. Skubiszewska-Zięba, R. Leboda, W. Janusz, V.M. Gun'ko, Effect of doping with copper (II) and nickel (II) oxides on morphological properties of silica/titania nanocomposites, Chem. Phys. Technol. Surf. 3 (2012) 386–394.
[41] M.A. Nazarkovsky, V.M. Gun'ko, V.I. Zarko, E. Skwarek, J. Skubiszewska-Zięba, R. Leboda, W. Janusz, Textural characteristics of SnO_2-doped titania/nanosilica and transition of phase of bound water, J. Chem. Technol. Metall. 48 (2013) 373–382.
[42] D. Fraga, R. Martí, I. Calvet, T. Stoyanova Lyubenova, L. Ladeira de Oliveira, J.B. Carda, Síntesis de kesterita

$Cu_2ZnSn(S,Se)_4$ mediante métodos de hot-injection y solvotermal, Bol. Soc. Esp. Ceram. Vidrio 53 (2014) 260–264.
[43] D. Fraga, R. Martí, T. Lyubenova, L. Oliveira, A. Rey, S. Kozhukharov, J. Carda, Solvothermal synthesis of CZTSSe for photovoltaic technology, Annual Proceedings of Angel Kanchev University of Ruse (Bulgaria) 51 (2012) 46–49.
[44] V. Kozhukharov, N. Brashkova, M. Ivanova, J. Carda, M. Machkova, Ceramic materials for SOFCs: current status, Bol. Soc. Esp. Cerám. Vidrio 41 (2002) 471–480.
[45] S. Simeonov, S. Kozhukharov, M. Machkova, N. Saliyski, V. Kozhukharov, Innovative methods and technologies for elaboration of SOFC ceramic materials (Review), J. Univ. Chem. Technol. Met. 47 (2012) 485–492.
[46] S. Simeonov, S. Kozhukharov, J.-C. Grenier, M. Machkova, V. Kozhukharov, Assessment of $Nd_{2-x}Sr_xNiO_{4-d}$ as a cathodic material for solid oxide fuel cell applications, J. Chem. Technol. Metall. 48 (2013) 104–110.
[47] S. Kozhukharov, Z. Nenova, T. Nenov, M. Machkova, V. Kozhukharov, Influencia de los suplementos de Ce(III)/(IV) sobre las características de los sensores de humedad con capas de TiO_2 preparadas mediante el método sol–gel, Bol. Soc. Esp. Cerám. Vidrio 52 (2013) 71–78.
[48] S. Somanescu, P. Osicaenu, J.-M.C. Moreno, L. Navarrete, J.-M. Serra, Mesoporous nanocomposite sensors based on $Sn_{1-x}Ce_xO_{2-\delta}$ metastable solid solution with high presence of Ce^{3+} valence state for selective detection of H_2 and CO, Microporous Mesoporous Mater. 179 (2013) 78–88.
[49] X.F. Liu, S.J. Huang, H.C. Gu, Crack growth behaviour of high strength aluminium alloy in 3.5%NaCl solution with corrosion inhibiting pigments, Int. J. Fatigue 24 (2002) 803–809.
[50] S. Kozhukharov, G. Tsaneva, V. Kozhukharov, J. Gerwann, M. Schem, T. Schmidt, M. Veith, Corrosion protection properties of composite hybrid coatings with involved nanoparticles of zirconia and ceria, J. Univ. Chem. Technol. Met. 43 (2008) 73–80.
[51] A. Huerta, R. Ordonez, H. Calderan, K. Tsuchiya, M. Umemoto, Production and sintering of $MgO–MgFe_2O_4$ powder ceramics by mechanical alloying, Depto de Ciencia de Materiales, Apdo, 2000, pp. 75–707.
[52] H. Heegn, H. Trinkler, H. Langbein, Phase formation and solid state structure on calcination of a nickel ferrite aceture precursor, Cryst. Res. Technol. 35 (2000) 1125–1132.
[53] H.V. Atkinson, A review of the role of short-circuit diffusion in the oxidation of nickel, chromium, and nickel-chromium alloys, Oxid. Met. 24 (1985) 177–178.
[54] A. Rahmel, W. Schwenk, Korrosion und Korrosionschutz von Stählen, Verlag Chemie, Weinheim, 1977, pp. 194–197.
[55] D. Landolt, Corrosion and Surface Chemistry of Metals, EPEL Press, 2007, pp. 385–387.
[56] P.E. López, J.B. Carda Castelló, E.C. Cordoncillo, Esmaltes y pigmentos cerámicos, Ed. Faenza Editrice Iberica s.l. I.S.B.N. 84-87683-19-3, pp. 196–198.